Accurate Force Field for Dimer Interactions: From Acetone to Dimethylsulfoxide

Luca Mancini[1(✉)], Andrea Lombardi[1,3], Fernando Pirani[2], Leonardo Pacifici[3], Marzio Rosi[2,3], and Noelia Faginas-Lago[1,3]

[1] Dipartimento di Chimica, Biologia e Biotecnologie, Università degli Studi di Perugia, 06123 Perugia, Italy
luca.mancini@unipg.it
[2] Dipartimento di Ingegneria Civile ed Ambientale, Università degli Studi di Perugia, 06125 Perugia, Italy
[3] Istituto CNR di Scienze e Tecnologie Chimiche "Giulio Natta", (CNR-SCITEC), 06123 Perugia, Italy

Abstract. Acetone (CH_3COCH_3) and dimethylsulfoxide (CH_3SOCH_3, DMS) are known for their peculiar properties and applications in different fields. The ability of acetone to dissolve an extensive number of chemical species with different physico-chemical properties makes this molecule an excellent solvent in various processes. On the other hand, due to its significant pharmacological potential, dimethylsulfoxide is regarded as an important species in medical chemistry and biology. Along with playing a crucial part in cryoprotection, it is also regarded as a significant species in the fields of radioprotection and anti-inflammatory medicine. For these reasons, the accurate analysis of the interaction between molecules, leading to the formation of dimers, trimers and clusters represents an important starting point for the detailed characterization of chemical properties of acetone and DMSO solutions. Within this framework, classical Molecular Dynamics simulations can be of great help to elucidate the main properties of the system and its behavior under the influence of different conditions. In this contribution we analyze the robustness of a new force field, developed for the acetone-acetone and DMSO-DMSO interaction, identified as a combination of electrostatic and non electrostatic contribution, the last one formulated using the *Improved Lennard-Jones* potential. A comparison with the data obtained through *Ab Initio* calculations allowed us to demonstrate the reliability of the developed force field.

Keywords: Acetone · Dimethylsulfoxide · Improved Lennard-Jones · Molecular Dynamics · Force Field

1 Introduction

Acetone is extremely soluble in water and may dissolve a variety of chemical compounds, including polar, nonpolar, and polymeric substances. These properties

© The Author(s), under exclusive license to Springer Nature Switzerland AG 2026
O. Gervasi et al. (Eds.): ICCSA 2025 Workshops, LNCS 15897, pp. 53–66, 2026.
https://doi.org/10.1007/978-3-031-97660-5_5

made acetone an useful and important solvent for different applications, ranging from laboratory studies to industrial processes [1,2]. Within the industrial framework, planning and increasing the effectiveness of technologically significant operations need a detailed understanding of the macroscopic and microscopic characteristics of acetone [3–5]. In the last years, different works have been performed in order to implement accurate force fields for the study of various systems involving acetone molecules. One example is represented by the analysis of complex mixtures, mainly composed of aldehides and chetones, to obtain important information of phase equilibrium properties [6–8]. Moreover, thermodinamic properties of liquid acetone were investigated through the use of classical molecular dynamics, obtaining a good agreement between theoretical predictions and experimental analysis [9]. Furthermore, given the high level of miscibility, the properties of acetone-water mixtures were extensively studied, including the effect of the variation of the dipole moment in acqueous solutions [10].

A similar molecule, dimethylsulfoxide (DMSO, CH_3SOCH_3), was analysed considering the analogies with acetone. The different chemical properties of sulfur, with respect to the carbon, are responsible for a different physical and chemical behavior of DMSO mixtures. Dimethylsulfoxide is particularly used in the field of cryopreservation, since it is not toxic and shows, together with a low molecular weight, a high solubility in acqueous solutions [11]. Being able to penetrate cell membranes, DMSO was proposed as cryopreservant for the preparation and storage of cells samples to be subjected to RNA sequencing [12]. Together with cryoprotective actions [13–15], DMSO also shows strong prophylactic and radioprotective properties [16]. Additional pharmacological applications of DMSO include anti-inflammatry and bacteriostatic activity, as well as analgesia [17]. One of the key aspects of the reactivity of both acetone and DMSO is related to their ability to form small aggregates and clusters [18]. Therefore, in order to unveil the reaction mechanism, a detailed understanding of the first step of the aggregation process, mainly driven by long-range non-covalent interactions, is pivotal.

A valid approach, considered as a satisfactory compromise between chemical accuracy and computational cost, is represented by classic molecular dynamics (MD) calculations. This last is regarded as a valuable technique for modeling the structure and predicting features of large systems, that are challenging or impossible to examine through precise *ab initio* research and/or experimental investigations. By using straightforward formulas based on Newton's laws of motion, molecular dynamics simulations enable the prediction of the positions of the various atoms in a system as a function of time. The most important step to be taken into account when setting the MD simulation is the implementation of the force field (FF), which describes the non covalent part of the interaction. The choice of the accurate parameters to describe the energy function is driven from both laboratory experiment and theoretical calculations. The electrostatic (Coulombic) contribution between atoms and the non-electrostatic one are the two primary components of MD force field, which is required to address non-covalent interactions. The proper modeling of intermolecular interactions (non-

electrostatic contribution), in particular the van der Waals component, which is always present and crucial for the overall dynamics, is one of the most difficult tasks in implementing accurate force fields.

In the last years, a new formulation of the intermolecular potential was presented to better take into account the effect of both long-range attraction and short-range repulsion. The formulation, named *Improved Lennard-Jones (ILJ)* [19], was obtained considering a sinergy between high level *ab initio* calculations and experimental investigations, performed through molecular beams scattering techniques [20–22]. A detailed description of the potential is reported in the next section (see Sect. 2.1 for details). One of the main advantages of the ILJ formulation is the relation with physical properties of the interacting systems, which gives a high level of transferability to the system. Recently, the same formulation was employed in different fields, ranging from astrochemistry [23,24] to material chemistry for energy applications [25,26]. It is also important to note that the *Improved Lennard-Jones* formulation, giving the first (force) and second (force constant) derivates in an analytical form, provides a physically grounded force field formulation, with a still limited computational cost.

In the present contribution, we report a comparison between the force field, developed through the ILJ formulation of the intermolecular potential, for the acetone-acetone interaction and the DMSO-DMSO one. A comparison with the data obtained via *ab initio* calculations is reported, in order to check the validity of the proposed potential. Previous analysis were already performed to study the interaction of acetone molecules in the formation of clusters [27] and to model the DMSO-water interaction [28]. The present work can indeed be considered as a continuation of the analysis already presented, with the aim of building a robust and appropriate potential functions.

2 Theoretical Methods

2.1 Potential Energy Surface for the Intermolecular Interactions

As already discussed, one of the key aspects for the correct execution of MD simulations is the accurate definition of the intermolecular interactions, which are essential components of the Force Field. In this work, we developed the Force Field taking into account that the total potential (V_{tot}) can be composed of two dominant contributions: the electrostatic potential (V_{elec}), evaluated in accordance with Coulomb's law, considering the atomic charges calculated for each molecule (reported in Fig. 1) and a second term (V_{nelec}), accounting for the non-electrostatic contribution of the interaction.

$$V_{tot}(r) = V_{elec} + V_{nelec} \tag{1}$$

This last term, V_{nelec}, was evaluated making use of the *Improved Lennard-Jones (ILJ)* model [19,27,29–31], associated to different molecular centers, each one identified as an effective atom - effective atom contribution, evaluated at a separation distance r. Accordingly, the total interaction is decomposed considering a series of pair-addictive contributions, which can be formulated taking into

account the strength of induced dipoles attraction and the average molecular sizes repulsion, and formulated as follows:

$$V_{nelec} = V_{ILJ} = \varepsilon \left[\frac{m}{n(r) - m} \left(\frac{r_m}{r} \right)^{n(r)} - \frac{n(r)}{n(r) - m} \left(\frac{r_m}{r} \right)^{m} \right] \tag{2}$$

where ε and r_m describes the well depth and its position, respectively, associated to each interaction pair, while m assumes the value of 6 in the case of neutral-neutral systems. The ε and r_m values are estimated on the basis of the molecular polarizabilty partition in components assigned to each interaction center. The newly implemented *n(r)* shows a dependence on the distance r, defined as:

$$n(r) = \beta + 4 \left(\frac{r}{r_m} \right)^2 \tag{3}$$

where the β parameter represents the hardness of the two interacting fragments, whose value can be properly modulated to indirectly include the role of further interaction components that can add to dispersion attraction and size repulsion effects. As a consequence, the ILJ potential may now enhance the Lennard-Jones function in asymptotic regions and it can indirectly include, through the modulation of the β parameter, for the perturbation effects due to additional interaction components as induction and charge transfer attractions.

2.2 Molecular Dynamics

In order to validate the efficiency of the Force Field, we run classical molecular dynamics simulations for both the dimethylsulfide and the acetone dimers. The DL_POLY [32] simulation package was used, considering the NVT ensamble, where the number of particles (N), volume (V) and temperature (T) are kept constant and using a Hoover-Nose thermostat [33] with a relaxation constant of 1 ps. After an initial equilibration period of 1 ns, all the simulations were performed for a total time of 3 ns, considering a pressure of 1 atm and for different values of temperature, ranging from 10 K to 300 K. Finally, the value of configurational energy (which refers to the potential energy associated to a specific configuration of the system), directly obtained from the OUTPUT of the MD calculations, was extrapolated to 0 K in order to compare the data with the results of *Ab Initio* calculations (see next section for details).

2.3 *Ab Initio* calculations

The final validation was performed considering the comparison between the results obtained from the MD calculations and the data coming from accurate electronic structure calculations. As already shown in several cases before [34–40], *ab initio* calculations based on DFT theory appear to be a good compromise between chemical accuracy and computational cost. Following this suggestion, using the *Gaussian09* [41] software, geometry optimization was performed at the

B3LYP [42,43] level of theory, with the inclusion of the Grimme's D3BJ dispersion [44] (B3LYP-D3). The 6-311++G(d,p) [45,46] basis set was used for this purpose, while single point energy calculations were performed with the same B3LYP-D3 functional with the more accurate aug-cc-pVTZ [47] basis set.

3 Results

3.1 Implementation of the Force Field

As a first step for the correct implementation of the ILJ interaction parameters, the dipole and/or quadrupole moments of the molecules in the gas phase must be accurately represented through the computation of atomic charges for the two interacting species. In Fig. 1, the atomic charges used to represent the dypole moment of the acetone and DMSO molecules are reported.

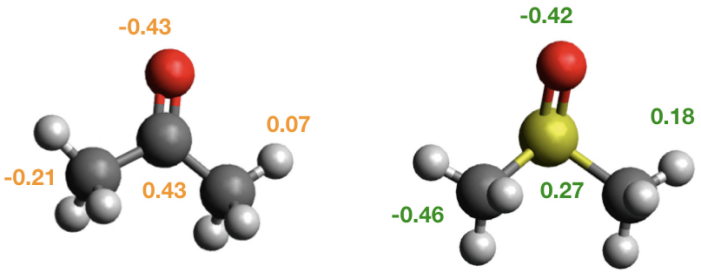

Fig. 1. Atomic charges used for the analysis of the electrostatic potential for both the acetone (left hand side) and the DMSO (right hand side) molecules.

The values shown in Fig. 1 are compatible with the experimental value of dipole moment for acetone and DMSO, which appears to be equal to 2.88 D and 3.96 D, respectively [48]. Additionally, the molecular polarizability, which represents a key properties for the determination of the ILJ parameters, is equal to 6.1 Å^3 for acetone [49] and 8.1 Å^3 for dimethylsulfoxide [28]. The values of the electric dipole moment and of the molecular polarizabilty of DMSO are greater than those of acetone, therefore we can expect considerable differences in the main interaction parameters for the DMSO dimer, with respect to those in acetone-acetone one. As already discussed (see Sect. 2 for details) the ILJ parameters are linked to the fundamental quantities related to the intermolecular potential [50], including the dipole moment (μ) and atomic/molecular polarizability (α). In details, the ε and r_m parameters for neutral-neutral systems are obtained as follows [51]:

$$r_m(\text{Å}) = 1.767 \frac{\alpha_1^{1/3} + \alpha_2^{1/3}}{(\alpha_1 \alpha_2)^{0.095}} \tag{4}$$

$$\varepsilon(meV) = 0.720 \frac{C_{6,eff}}{r_m^6} \tag{5}$$

where $C_{6,eff}$ is the long-range attraction coefficient, evaluated considering the number of electrons, effectively undergoing polarization, of the two interacting particles (expressed as N_1 and N_2)

$$C_{6,eff}(meV\text{Å}^6) = 15700 \frac{\alpha_1 \alpha_2}{\left(\frac{\alpha_1}{N_1}\right)^{1/2} + \left(\frac{\alpha_2}{N_2}\right)^{1/2}} \tag{6}$$

The direct relation between the ILJ parameters and physical properties of the interacting system leads to a high degree of transferability, allowing to move easily from a system to a similar one, without particular changes in the parameters. Additionally, the derived parameters lead to a high level of portability of the formulation, allowing also to study complex systems, by simply decomposing the main molecular structure in different moieties. Considering the relations previously presented, the ILJ parameters for the interaction between two acetone molecules, as well as the ones for the DMSO-DMSO, were calculated. The final parameters are reported in Tables 1 and 2, respectively.

Table 1. List of the Improved Lennard-Jones parameters (well depth, ε, and equilibrium distance, r_m) evaluated for the acetone-acetone system. (Adapted from the work presented by N. Faginas-Lago et al. [27])

Interacting Pair	r_m (Å)	ε (kcal/mol)
C_{CH_3} - C_{CH_3}	4.053	0.262
C_{CO} - C_{CO}	3.628	0.150
O - O	3.398	0.119
C_{CO} - O	3.521	0.130

Table 2. List of the Improved Lennard-Jones parameters (well depth, ε, and equilibrium distance, r_m) evaluated for the DMSO-DMSO system. (Adapted from the work presented by L. Mancini et al. [28])

Interacting Pair	r_m (Å)	ε (kcal/mol)
C_{CH_3} - C_{CH_3}	4.053	0.262
S - S	4.075	0.325
O - O	3.534	0.150
S - O	3.847	0.201

As can be seen, the ε parameter for the DMSO-DMSO interaction assumes, in general, values different from those derived for the acetone dimer, especially the

ones associated to the interaction pairs involving the sulfur atom are significantly higher. This reflects the higher value of the molecular polarizability of DMSO, with respect to the case of acetone itself. The β parameter can be appropriately modulated in the V_{elec} changes and is typically thought to be in the range of 8.5 $\pm$ 2.5. Furthermore, other distinct contributions that are less significant and not directly included in the formulation–such as additional additive components of the interaction at long distances that are indirectly included–can be compensated for and included using the same parameter.

3.2 Validation of the Force Field

In order to assess the viability of the developed force field for both the dimer interactions, we run MD calculations, as outlined in Sect. 2.2. As a first step, we evaluated the interaction energy of the dimer by performing MD calculations at different temperatures and extrapolating the value of the configurational (or potential) energy (E_{cfg}) at 0 K. It is possible to consider this last value as an estimate of the binding energy. In Fig. 2 the values of E_{cfg} obtained for the acetone dimer at different temperatures (represented by the marked points) are shown, together with the linear extrapolation (dashed line) used to obtain the value at 0 K. Our results predict a configurational energy of - 4.92 kcal/mol.

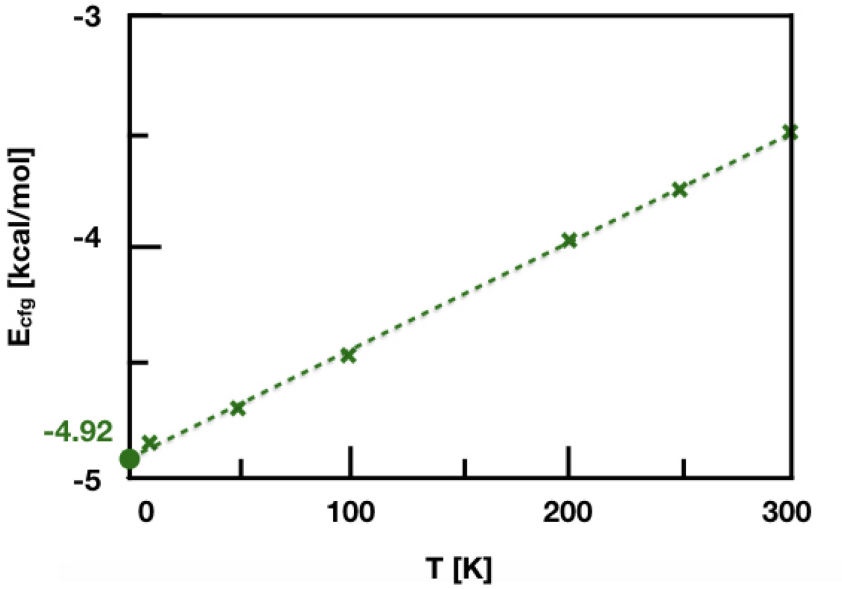

Fig. 2. Configurational energy (E_{cfg}) as a function of the temperature for the acetone dimer.

This value can be directly compared with the data obtained by *ab initio* calculations. The analysis performed at the B3LYP-D3/aug-cc-pVTZ level of theory lead to a value of energy of -5.89 kcal/mol, in agreement with the data obtained extrapolating MD results. A similar procedure was carried out for the case of the DMSO dimer. The results obtained from the analysis performed through classical MD simulations are reported in Fig. 3, obtaining a value of configurational energy at a temperature of 0 K equal to - 10.35 kcal/mol.

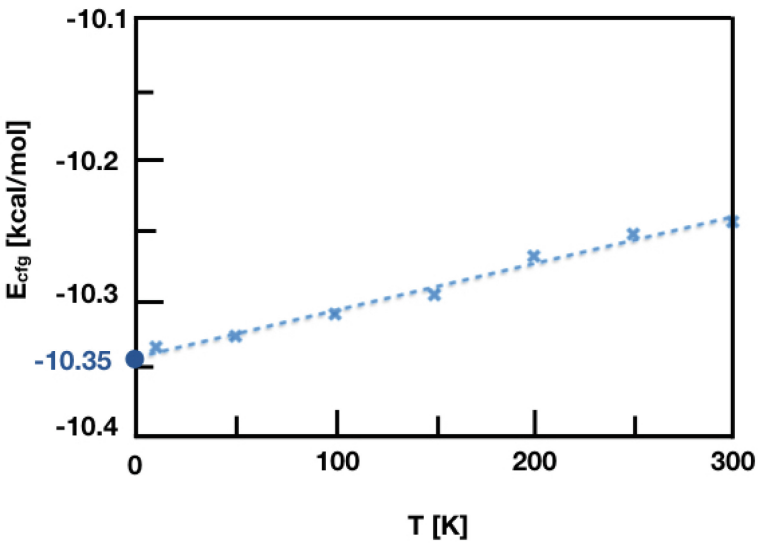

Fig. 3. Configurational energy (E_{cfg}) as a function of the temperature for the DMSO dimer.

Also in this case, the value can be compared with the data obtained at the B3LYP-D3/aug-cc-pVTZ level of theory, which reported a value of energy of -11.4 kcal/mol, showing once again the agreement between classical MD predictions and *ab initio* calculations, within the range of accuracy due to the different types of calculations. In Table 3 are reported the energies obtained through classical MD calculation and *ab initio* analysis for a direct comparison.

Table 3. Electrostatic (E_{coul}), non-electrostatic (E_{ILJ}) and configurational (potential) energy (E_{cfg}), in kcal/mol, obtained from the extrapolation at 0 K from classical MD calculations E_{cfg} compared with the *ab initio* energy, evaluated at the B3LYP-D3/aug-cc-pVTZ level of theory E_{B3LYP} for both the acetone and DMSO dimer.

Dimer	MD			*Ab initio*
	E_{coul}	E_{ILJ}	E_{cfg}	$E_{B3LYP-D3}$
Acetone-Acetone	−2.82	−2.08	−4.92	−5.89
DMSO-DMSO	−7.99	−2.32	−10.35	−11.4

As can be noticed from the data reported in Table 3, the interaction energy is higher for the DMSO dimer, with respect to the case of acetone. The reason of such a difference is related to both the electrostatic contribution of the interaction, due to the higher value of dipole moment of DMSO, and the non-electrostatic contribution, since the value of polarizability of DMSO is considerably higher than the one of acetone.

Finally, a comparison between the geometry of the adducts can be performed in order to assess the force field used to describe the intermolecular forces. In details, the geometry obtained from the last frame of the trajectory carried out at 10 K was used as a starting point for a geometry optimization, carried out at the B3LYP-D3/6-311++G(d, p) level of theory. In Table 4 the main atom-atom distances for both the acetone dimer and the DMSO dimer are reported, while Fig. 4 shows a 3D representation of the structure of the dimer for both acetone and DMSO.

Table 4. Main atom-atom distances for both the acetone dimer and the DMSO dimer, resulting from MD calculations and DFT (B3LYP-D3/6-311++G(d,p) level of theory.

Atom-Atom	r_{MD} (Å)	r_{DFT} (Å)
Acetone-Acetone		
C_{CO}-C_{CO}	3.746	3.222
O-O	3.953	3.495
C_{CH_3}-C_{CH_3}	3.840	3.907
DMSO-DMSO		
S-S	4.450	4.390
O-O	3.963	3.498
C_{CH_3}-C_{CH_3}	3.677	3.943

As can be seen from the data reported in Table 4, the values of distances between the two molecules of each dimer derived from MD calculations are comparable with the DFT data. The main deviations are lower than 0.52 Å for the acetone dimer and lower than 0.47 Å for the DMSO-DMSO interaction, pointing

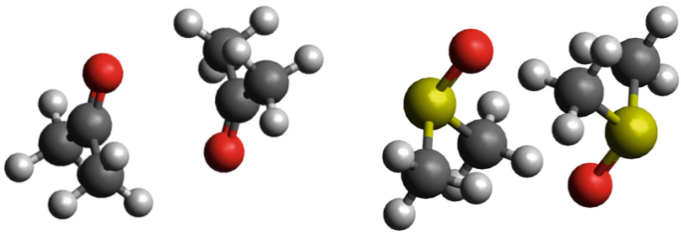

Fig. 4. 3D representation of the structure of the dimer for acetone (left) and DMSO (right) optimized at the B3LYP-D3/6-311++G(d, p) level of theory.

out a good agreement between the two methods and, therefore, confirming the validity and robustness of the presented force field.

4 Conclusions

The development of accurate force fields, which determines the interaction energy and the geometry associated to the dimers aggregation, represents a crucial first step of relevance for the formation of liquids and solutions. In particular, we presented the parameters for the ILJ formulation of the long-range potential for both the acetone-acetone and the DMSO-DMSO interactions. Moreover, the binding energies obtained for the DMSO dimer appear to be significantly stronger than the ones between acetone molecules. This finding is a direct consequence of the higher value of the molecular polarizability and electric dipole of DMSO with respect to those of acetone. The data obtained performing classical MD simulations were compared with the results of DFT calculations, showing a general good agreement of both the configurational energy and the final geometry of the system, considering the main differences in the two approaches. Further refinement of the ILJ parameters can be considered in order to get a better agreement with the *ab initio* data. In particular, a fine-tuning of the β parameter can be useful for the purpose. It is possible to conclude, therefore, that the present work sets the stage for a more complex analysis and the parameters used for the formulation of both the electrostatic and non-electrostatic components of the interactions are reasonable and can be used for the development of the force field. An additional analysis will be performed in the case of bulk systems, which will be the purpose of a future work, where the outcome of the MD calculations will be compared with physico-chemical properties of teh system. Additionally, more accurate *ab initio* calculations will be performed at a higher level of theory in order to set reference data for the complete validation of the force field. The same strategy can be applied to the study of different systems, with a wide range of applications, including the study of nanomaterials for energy storage and carbon neutrality techniques, allowing to properly describe the interaction of small molecules with adsorbing substrates.

Acknowledgments. This work has been funded by the European Union - NextGenerationEU under the Italian Ministry of University and Research (MUR) National Innovation Ecosystem grant ECS00000041 - VITALITY - CUP J97G22000170005. LP acknowledges financial support from the European Union - Next Generation EU, National Centre for HPC, Big Data and Quantum Computing – HPC project - Centro Nazionale – CN0000013: CUP:B93C22000620006

Disclosure of Interests. The authors have no competing interests to declare that are relevant to the content of this article.

References

1. Nagai, K.: Appl. Catal., A: Gen. **221**, 367 (2001)
2. Uglea, C.V., Negulescu, I.I.: Synthesis and Characterization of Oligomers. CRC Press (1991)
3. Asada, M., Fujimori, T., Fujii, K., Kanzaki, R., Umebayashi, Y., Ishiguro, S.I.: Solvation structure of magnesium, zinc, and alkaline earth metal ions in n, n-dimethylformamide, n, n-dimethylacetamide, and their mixtures studied by means of Raman spectroscopy and DFT calculations–ionic size and electronic effects on steric congestion. J. Raman Spectrosc.: Int. J. Original Work Aspects Raman Spectrosc. Includ. High. Order Process. Brillouin Rayleigh Scatter. **38**(4), 417–426 (2007)
4. Palombo, F., Paolantoni, M., Sassi, P., Morresi, A., Giorgini, M.G.: Molecular dynamics of liquid acetone determined by depolarized Rayleigh and low-frequency Raman scattering spectroscopy. Phys. Chem. Chem. Phys. **13**(36), 16197–16207 (2011)
5. Mollner, A.K., Brooksby, P.A., Loring, J.S., Bako, I., Palinkas, G., Fawcett, W.R.: Ion- solvent interactions in acetonitrile solutions of lithium iodide and tetrabutylammonium iodide. J. Phys. Chem. A **108**(16), 3344–3349 (2004)
6. Ferrando, N., Lachet, V., Boutin, A.: Monte Carlo simulations of mixtures involving ketones and aldehydes by a direct bubble pressure calculation. J. Phys. Chem. B **114**(26), 8680–8688 (2010)
7. Stubbs, J.M., Potoff, J.J., Siepmann, J.I.: Transferable potentials for phase equilibria. 6. United-atom description for ethers, glycols, ketones, and aldehydes. J. Phys. Chem. B **108**(45), 17596–17605 (2004)
8. Hantal, G., Jedlovszky, P., Hoang, P.N., Picaud, S.: Investigation of the adsorption behaviour of acetone at the surface of ice. A grand canonical Monte Carlo simulation study. Phys. Chem. Chem. Phys. **10**(42), 6369–6380 (2008)
9. Ghatee, M.H., Taslimian, S.: Investigation of temperature and pressure dependent equilibrium and transport properties of liquid acetone by molecular dynamics simulation. Fluid Phase Equilib. **358**, 226–232 (2013)
10. Pereyra, R.G., Asar, M.L., Carignano, M.A.: The role of acetone dipole moment in acetone-water mixture. Chem. Phys. Lett. **507**(4–6), 240–243 (2011)
11. Lovelock, J.E., Bishop, M.W.: Prevention of freezing damage to living cells by dimethyl sulphoxide. Nature **183**(4672), 1394–1395 (1959)
12. Wohnhaas, C.T., et al.: DMSO cryopreservation is the method of choice to preserve cells for droplet-based single-cell RNA sequencing. Sci. Rep. **9**(1), 10699 (2019)
13. Chaytor, J.L., et al.: Inhibiting ice recrystallization and optimization of cell viability after cryopreservation. Glycobiology **22**(1), 123–133 (2012)

14. Wolfe, J., Bryant, G.: Freezing, drying, and/or vitrification of membrane-solute-water systems. Cryobiology **39**(2), 103–129 (1999)
15. Wolfe, J., Bryant, G.: Cellular cryobiology: thermodynamic and mechanical effects. Int. J. Refrig **24**(5), 438–450 (2001)
16. Jacob, S.W., Herschler, R.: Pharmacology of DMSO. Cryobiology **23**(1), 14–27 (1986)
17. Pope, D., Oliver, W.: Dimethyl sulfoxide (DMSO). Can. J. Comp. Med. Vet. Sci. **30**(1), 3 (1966)
18. Malloum, A., Conradie, J.: Non-covalent interactions in dimethylsulfoxide (DMSO) clusters and DFT benchmarking. J. Mol. Liq. **350**, 118522 (2022)
19. Pirani, F., Brizi, S., Roncaratti, L.F., Casavecchia, P., Cappelletti, D., Vecchiocattivi, F.: Beyond the lennard-jones model: a simple and accurate potential function probed by high resolution scattering data useful for molecular dynamics simulations. Phys. Chem. Chem. Phys. **10**(36), 5489–5503 (2008)
20. Pirani, F., Maciel, G.S., Cappelletti, D., Aquilanti, V.: Experimental benchmarks and phenomenology of interatomic forces: open-shell and electronic anisotropy effects. Int. Rev. Phys. Chem. **25**(1–2), 165–199 (2006)
21. Pirani, F., Albertı, M., Castro, A., Teixidor, M.M., Cappelletti, D.: Atom-bond pairwise additive representation for intermolecular potential energy surfaces. Chem. Phys. Lett. **394**(1–3), 37–44 (2004)
22. Cappelletti, D., Ronca, E., Belpassi, L., Tarantelli, F., Pirani, F.: Revealing charge-transfer effects in gas-phase water chemistry. Acc. Chem. Res. **45**(9), 1571–1580 (2012)
23. Richardson, V., et al.: Fragmentation of interstellar methanol by collisions with He^+: an experimental and computational study. Phys. Chem. Chem. Phys. **24**(37), 22437–22452 (2022)
24. Mancini, L., et al.: Destruction of interstellar methyl cyanide CH_3CN via collisions with He^+ ions. Astron. Astrophys. **691**, A83 (2024)
25. Apriliyanto, Y.B., Faginas Lago, N., Lombardi, A., Evangelisti, S., Bartolomei, M., Leininger, T., Pirani, F.: Nanostructure selectivity for molecular adsorption and separation: the case of graphyne layers. J. Phys. Chem. C **122**(28), 16195–16208 (2018)
26. Faginas-Lago, N., Apriliyanto, Y.B., Lombardi, A.: Confinement of CO_2 inside carbon nanotubes. Eur. Phys. J. D **75**(5), 161 (2021)
27. Faginas Lago, N., Albertí, M., Lombardi, A., Pirani, F.: A force field for acetone: the transition from small clusters to liquid phase investigated by molecular dynamics simulations. Theoret. Chem. Acc. **135**, 1–9 (2016)
28. Mancini, L., Lombardi, A., Pirani, F., Pacifici, L., Rosi, M., Faginas-Lago, N.: A computational analysis of the DMSO-water interaction: toward the implementation of an accurate force field. In: International Conference on Computational Science and Its Applications, pp. 361–374. Springer (2024)
29. Lombardi, A., Laganà, A., Pirani, F., Palazzetti, F., Faginas-Lago, N.: Carbon oxides in gas flows and earth and planetary atmospheres: state-to-state simulations of energy transfer and dissociation reactions. In: LNCS, PART 2, vol. 7972, pp. 17–31 (2013). https://doi.org/10.1007/978-3-642-39643-4_2
30. Lombardi, A., Faginas-Lago, N., Gaia, G., Federico, P., Aquilanti, V.: Collisional energy exchange in CO_2–N_2 gaseous mixtures. In: Gervasi, O., et al. (eds.) ICCSA 2016. LNCS, vol. 9786, pp. 246–257. Springer, Cham (2016). https://doi.org/10.1007/978-3-319-42085-1_19

31. Albertí, M., Faginas-Lago, N.: Ion size influence on the AR solvation shells of $M^+C_6F_6$ clusters (M = Na, K, Rb, Cs). J. Phys. Chem. A **116**(12), 3094–3102 (2012). https://doi.org/10.1021/jp300156k
32. Smith, W., Yong, C., Rodger, P.: Dl_poly: application to molecular simulation. Mol. Simul. **28**(5), 385–471 (2002)
33. Hoover, W.G.: Canonical dynamics: equilibrium phase-space distributions. Phys. Rev. A **31**(3), 1695 (1985)
34. Pannacci, G., et al.: A combined crossed molecular beam and theorerical study of the O(^{3}P, ^{1}D) + acrylonitrile (CH_2CHCN) reactions and implications for combustion and extraterrestrial environments. Phys. Chem. Chem. Phys. **25**(30), 20194–20211 (2023)
35. Liang, P., et al.: OH $(2\pi)+$ C_2H_4 reaction: a combined crossed molecular beam and theoretical study. J. Phys. Chem. A **127**(21), 4609–4623 (2023)
36. Rosi, M., et al.: Electronic structure and kinetics calculations for the $Si+SH$ reaction, a possible route of SiS formation in star-forming regions. In: Computational Science and Its Applications–ICCSA 2019: 19th International Conference, Saint Petersburg, Russia, 1–4 July 2019, Proceedings, Part III 19, pp. 306–315. Springer (2019)
37. Liang, P., et al.: Combined crossed molecular beams and computational study on the $N(^2D) + HCCCN(X^1\Sigma^+)$ reaction and implications for extra-terrestrial environments. Mol. Phys. **120**(1–2), e1948126 (2022)
38. Vanuzzo, G., et al.: The N (^2D) + CH_2CHCN (vinyl cyanide) reaction: a combined crossed molecular beam and theoretical study and implications for the atmosphere of titan. J. Phys. Chem. A **126**(36), 6110–6123 (2022)
39. Vanuzzo, G., et al.: Reaction N (^2D) + CH_2CCH_2 (allene): an experimental and theoretical investigation and implications for the photochemical models of titan. ACS Earth Space Chem. **6**(10), 2305–2321 (2022)
40. Recio, P., et al.: A crossed molecular beam investigation of the N (^2D) + pyridine reaction and implications for prebiotic chemistry. Chem. Phys. Lett. **779**, 138852 (2021)
41. Frisch, M., et al.: Fox: Gaussian 09, Revision A. 02, 2009. Gaussian. Inc., Wallingford (2009)
42. Becke, A.D.: Density functional thermochemistry. III. The role of exact exchange. J. Chem. Phys. **98**(7), 5648–5652 (1993). https://doi.org/10.1063/1.464913
43. Stephens, P.J., Devlin, F.J., Chabalowski, C.F., Frisch, M.J.: *Ab Initio* calculation of vibrational absorption and circular dichroism spectra using density functional force fields. J. Phys. Chem. **98**(45), 11623–11627 (1994). https://doi.org/10.1021/j100096a001
44. Grimme, S., Ehrlich, S., Goerigk, L.: Effect of the damping function in dispersion corrected density functional theory. J. Comput. Chem. **32**(7), 1456–1465 (2011)
45. Krishnan, R., Binkley, J.S., Seeger, R., Pople, J.A.: Self-consistent molecular orbital methods. XX. A basis set for correlated wave functions. J. Chem. Phys. **72**(1), 650–654 (1980)
46. McLean, A., Chandler, G.: Contracted gaussian basis sets for molecular calculations. I. Second row atoms, z= 11–18. J. Chem. Phys. **72**(10), 5639–5648 (1980)
47. Dunning Jr., T.H.: Gaussian basis sets for use in correlated molecular calculations. I. the atoms boron through neon and hydrogen. J. Chem. Phys. **90**(2), 1007–1023 (1989). https://doi.org/10.1063/1.456153
48. Nelson, R., Lide, D., Margott, A.: Selected values of electric dipole moments for molecules in the gas phase NSRDS-NBS10. Washington, DC (1967)

49. Olney, T.N., Cann, N., Cooper, G., Brion, C.: Absolute scale determination for photoabsorption spectra and the calculation of molecular properties using dipole sum-rules. Chem. Phys. **223**(1), 59–98 (1997)
50. Maitland, G., Rigby, M., Smith, E., Wakeham, W., Henderson, D.: Intermolecular forces: their origin and determination (1987)
51. Cambi, R., Cappelletti, D., Liuti, G., Pirani, F.: Generalized correlations in terms of polarizability for van der Waals interaction potential parameter calculations. J. Chem. Phys. **95**(3), 1852–1861 (1991)